# Control and diagnostic uses of feedback

Cite as: Physics of Plasmas **7**, 1759 (2000); https://doi.org/10.1063/1.873996
Submitted: 17 November 1999 . Accepted: 14 January 2000 . Published Online: 19 April 2000

A. K. Sen

# Control and diagnostic uses of feedback*

A. K. Sen[†,a)]
*Plasma Physics Laboratory, Columbia University, New York, New York 10027*

(Received 17 November 1999; accepted 14 January 2000)

Recent results on multimode feedback control of magnetohydrodynamic (MHD) modes and a variety of diagnostic uses of feedback are summarized. First, is the report on reduction and scaling of transport under feedback. By controlling the fluctuation amplitudes and consequently the transport via feedback, it is found that the scaling of the diffusion coefficient is linear with root-mean-square rms fluctuation level. The scaling appears not to agree with any generic theory. A variety of other diagnostic uses of feedback have been developed. The primary goal is an experimental methodology for the determination of dynamic models of plasma turbulence, both for better transport understanding and more credible feedback controller designs. A specific motivation is to search for a low-order dynamic model, suitable for the convenient study of both transport and feedback. First, the time series analysis method is used for the determination of chaotic attractor dimension of plasma fluctuations. For $\mathbf{E}\times\mathbf{B}$ rotational flute modes it is found to be close to three, indicating that a low-order dynamic model may be adequate for transport prediction and feedback controller design. Second, a new method for direct experimental determination of nonlinear dynamical models of plasma turbulence using feedback has been developed. Specifically, the process begins with a standard three-wave coupling model and introduces a variable feedback gain. The power spectrum, delayed power spectrum, and bispectrum of fluctuations are then experimentally obtained. By varying the feedback gain continuously, an arbitrary number of numerical equations for a fixed number of unknowns can be generated. Their numerical solution yields the linear dispersion, as well as nonlinear coupling coefficients. This method has been successfully applied for $\mathbf{E}\times\mathbf{B}$ rotationally driven flute modes. © *2000 American Institute of Physics.* [S1070-664X(00)92705-8]

## I. INTRODUCTION

### A. Motivation

It is well known that all plasmas suffer from fluctuations caused by instabilities, irrespective of the types of devices and systems and their intended applications. The deleterious consequences of these fluctuations are many: nonuniformity, strongly increased transport, and if violent enough, a macroscopic breakup. Therefore, elimination or reduction of those instabilities and consequent fluctuations and transport is a highly desirable goal with great promise.

Control science is a very well developed discipline which has played critical roles in all manners of industrial products and processes, and many frontiers of modern technology. However, its theoretical foundations and experimental methodologies are nearly exclusively valid for lumped parameter systems characterized by ordinary differential equations. As such these are not applicable to distributed parameter systems like plasmas, characterized by partial differential equations. This may have caused severe neglect of research in the control of plasma instabilities and fluctuations. In the past, we have attempted to extend, adapt, and extrapolate the theoretical and experimental tools of modern control science with some success.[1–11] In this paper we summarize some of our recent theoretical and experimental research in this area.

### B. Fundamental issues and outline of the paper

An important unsolved problem in this area is a suitable remote suppressor which will avoid unacceptable intrusion into a hot plasma by metallic probes or electrodes as suppressors. Experimentally in the Columbia Linear Machine (CLM), we have solved this problem by developing an ion/electron beam suppressor,[4,5] which is extrapolatable to fusion machines as neutral beam suppressors.[9] The other important problem is the simultaneous suppression of many modes of plasma instabilities. This is a system theoretic problem in control science whose solution can be adapted to plasma systems. Both of the above issues are jointly addressed in the next section of this paper.

In Sec. III of the paper we develop novel diagnostics tools for plasma turbulence based on feedback. The key idea is that linear feedback can modify the dynamic behavior of a plasma, but not its equilibrium parameters. This allows the use of a variable feedback in experimental observations of changes in the dynamic behavior of the plasma, which are direct functions of feedback gains. This property allows qualitative and quantitative inference about the dynamical model of the plasma turbulence. This subject is elaborated on in Sec. III.

*Paper UI2 6 Bull. Am. Phys. Soc. **44**, 291 (1999).
[†]Invited speaker.
[a)]In collaboration with J. S. Chiu.

 

## II. CONTROL OF MULTIMODE MHD INSTABILITIES VIA NEUTRAL BEAM FEEDBACK

It is widely believed that magnetohydrodynamic (MHD) instabilities seriously degrade confinement in magnetic fusion devices like tokamaks and RFP's (reversed field pinches). In RFP's these have large amplitudes and pose a serious limit on confinement. In tokamaks, these can result in minor disruptions, causing confinement degradation and occasionally major disruptions which can cause serious damage. From both experimental and theoretical work it appears that often only a few discrete MHD modes are implicated. Interesting and promising results using magnetic coil suppressors for a single MHD mode have been reported.[12–15] However, neutral beam suppressors may have some advantages, especially when the modes are located deep in the plasma, e.g., a $m=1$, $n=1$ MHD mode. The stabilization of a single ideal MHD mode ($m=2,n=1$)[16] or a single tearing mode ($m=1,n=1$)[17] via a neutral beam suppressor has been discussed before. However, when one mode is stabilized another mode is often destabilized, [18,19] as mentioned before. Furthermore, there may be need for stabilization of several unstable modes. Therefore we consider simultaneous stabilization of several MHD modes, without destabilization of any other via the following control system design methodology.

### A. Model equation of multimode MHD instabilities

One can write the linearized ideal MHD equations in the following well-known form with the inclusion of a momentum input from the neutral beam:

$$\rho\frac{\partial^2\boldsymbol{\xi}}{\partial t^2}=\mathbf{F}(\boldsymbol{\xi})+\frac{d\mathbf{M}}{dt}, \tag{1}$$

where $\rho$, $\boldsymbol{\xi}$, and $\mathbf{M}$ are the equilibrium density, perturbed plasma displacement, and momentum imparted by the neutral beam, respectively, and $\mathbf{F}(\boldsymbol{\xi})$ is the usual MHD force operator. The momentum input $\mathbf{M}$ can be written as[16]

$$\frac{dM_r}{dt}=n_b m_b V_b^2 N_0(\sigma_e+\sigma_i+\sigma_x), \tag{2}$$

where $N_0$, $\sigma_e$, $\sigma_i$, and $\sigma_x$ are plasma density and ionization cross sections via electron, ion impacts, and charge exchange, respectively. We assume that the homogeneous problem of Eq. (1) without the feedback term has been completely solved to yield the eigenfunctions $\xi_k$ and the eigenfrequencies (growth, damping rates) $\gamma_k$. Then one can expand the perturbed plasma displacement $\xi$ in terms of the eigenfunctions as

$$\boldsymbol{\xi}=\sum a_k\boldsymbol{\xi}_\mathbf{k},$$

where $a_k$ is the modal amplitude. We substitute this expansion in Eq. (1), take the scalar product of both sides with $\xi_k^*$, and obtain

$$\ddot{a}_k=\gamma_k^2 a_k+\int \boldsymbol{\xi}_\mathbf{kr}^* f(\mathbf{r})\dot{M}_r(t)dV/\rho,$$

where $f(\mathbf{r})$ characterizes the localized structure of the neutral beam momentum input in Eq. (1) and an overdot indicates time derivative. We expand the structure function $f(\mathbf{r})$ in terms of the orthonormal eigenfunctions shown above as

$$f(r)=\sum_{k>0} b_k\boldsymbol{\xi}_\mathbf{kr},$$

and substitute it in the above equation to obtain

$$\ddot{a}_k=\gamma_k^2 a_k+b_k M_k(t)/\rho,$$
$$M_k(t)=n_{bk}(t)m_b V_b^2 N_0(\sigma_e+\sigma_i+\sigma_x). \tag{3}$$

We now write Eq. (3) as two first-order equations in two modal amplitudes and after several linear transformations obtain

$$\begin{bmatrix}\dot{a}_{k_1}\\ \dot{a}_{k_2}\end{bmatrix}=\begin{bmatrix}\gamma_k & 0\\ 0 & -\gamma_k\end{bmatrix}\begin{bmatrix}a_{k_1}\\ a_{k_2}\end{bmatrix}+\begin{bmatrix}b_k M_k/\rho\gamma_k\\ b_k M_k/\rho\gamma_k\end{bmatrix}. \tag{4}$$

In the above equation the growth $\gamma_k$ and damping rate $-\gamma_k$ for the conjugate MHD modes with amplitudes $a_{k_1}$ and $a_{k_2}$ are explicitly shown. We can now write Eq. (4) for $N$ mode pairs in the following matrix form and use $c(t)$ as the control signal with coupling coefficients $\alpha_k$ to the mode $k$ as

$$[\ddot{a}]=[A][a]+[\alpha]c(t),\quad [\alpha]=[\ldots\alpha_k\alpha_k\ldots]^T;$$
$$\alpha_k=(b_k M_k/\rho\gamma_k), \tag{5}$$

where superscript $T$ stands for matrix transpose. The modal feedback is now implemented via generation of the single control signal $c(t)$ via a gain matrix $[G]$ as follows:

$$c(t)=[G]^T[a]/a_0, \tag{6}$$

where $[G]$ is a column matrix defined as $[G]^T=[\ldots G_{k_1},G_{k_2}\ldots]$. Substituting Eq. (6) into Eq. (5) we obtain

$$[\dot{a}]=([A]+[\alpha][G]^T/a_0)[a].$$

For $[a]\sim e^{-i\omega t}$, we find the controlled dispersion relation from the above equation to be

$$\|i\omega[I]+[A]+[\alpha][G]^T/a_0\|=0, \tag{7}$$

where $\|$ denotes the determinant of a matrix. The dispersion relation can also be written as a polynomial of order $2N$ in $\omega$, say as follows:

$$\omega^{2N}+\sum_{i=0}^{2N-1} h_i(G_k)\omega^i=0, \tag{8}$$

where $h_i$ are the coefficients of the polynomial which are functions of the gains $G_k$. We now suppose that we desire to neutrally stabilize all the modes with the growth rate $+\gamma_k$ and leave all their conjugate partners with the decay rate $-\gamma_k$ unaltered. Then the desired dispersion relation will be

$$\Pi_{k=1}^{N}\omega(\omega+i\gamma_k)=\omega^{2N}+\sum_{i=0}^{2N_1} d_i(\gamma_k)\omega^i=0, \tag{9}$$

which is essentially a definition of the coefficients $d_i$ of the polynomial in $\omega$ of degree $2N$, and $d_i$ are functions of growth rate $\gamma_k$ only. Equating Eqs. (8) and (9) yields $2N$ algebraic equations for $2N$ unknown $G_{k_1},G_{k_2}$'s. Solution of these equations gives the required modal feedback gains. The second important question is the lack of direct experimental

access to all the modes individually, which is assumed in the above formalism. This can be achieved via unscrambling all the mode information from a single sensor (like Mirnov coil or soft x-ray diode) signal with the help of an electronic circuit called ''State Reconstruction.'' This has been discussed before by utilizing a Luernberger-type[20] circuit. A convenient scheme based on the above concept, but with a far simpler formalism, has been implemented experimentally with great success. In this scheme, additional ''states'' were generated via differentiation of the single sensor signal, followed by a state feedback to stabilize simultaneously an $\mathbf{E}\times\mathbf{B}$ rotationally driven and an ion temperature gradient mode.[6]

## III. DIAGNOSTIC USES OF FEEDBACK

Almost by definition linear feedback can modify the dynamic behavior of plasma, but not its equilibrium parameters. We have repeatedly verified this proposition in many experiments. The change in the dynamic behavior of plasma is a direct function of the change in feedback gains. This property immediately makes it possible to infer about a dynamical model of the plasma. We develop this approach theoretically and experimentally into a plasma diagnostic technique for the experimental determination of a dynamical model of plasma. More directly, one can suppress plasma fluctuations to a significant degree (not completely) and reduce the corresponding transport. Furthermore, we suppose that one has an experimental control parameter which can vary the drive of the instability. Then one can determine a scaling law between the transport and the fluctuation level. Lastly one can perform this experiment without and with feedback and compare the respective transport scalings. As linear feedback affects only the linear drive and not the nonlinear dynamics, but transport depends on both, the comparison will shed light on the nonlinear physics. These methodologies are described below. All experiments were performed in the Columbia Linear Machine[21] (CLM) and the instability studied is an $\mathbf{E}\times\mathbf{B}$ rotationally driven electrostatic flute mode.[22]

### A. A study of transport scaling using feedback

We focus on the measurement of density transport due to the $\mathbf{E}\times\mathbf{B}$ fluctuations and its scaling.[23] The feedback loop consists of the plasma, a sensor which is a Langmuir probe biased to collect ion saturation current, a suppressor which is a small modulated electron beam and a feedback amplifier gain, and a phase shifter as shown in Fig. 1. It is assumed that the density $\tilde{n}$ and electric potential $\tilde{\phi}_p$ of this flute-like electrostatic instability have the form proportional: $\tilde{n},\tilde{\phi}_p \sim f(r)e^{i(m\theta-\omega t)}$ in a cylindrical plasma with coordinates $r$, $\theta$, $z$, and $m$ and $\omega$ are azimuthal mode number and frequency of the mode, respectively. The anomalous radial particle flux is

$$\Gamma=\mathbf{Re}\{\tilde{v}_r\tilde{n}\rangle\}=\frac{m}{rB}\mathbf{Re}\{i\langle\tilde{\phi}\tilde{n}\rangle\}=\frac{m}{rB}\int|P_{\Phi N}|\sin\Theta_{\Phi N}df, \tag{10}$$

where $v_r$, $B$, $P_{\Phi N}$, $\Theta_{\Phi N}$, and $f$ are radial velocity due to $-\nabla\phi\times\mathbf{B}/B^2$ motion, axial magnetic field, cross-power spectrum and relative phase spectrum of $\tilde{\phi}_p$ and $\tilde{n}$, and frequency, respectively. Then the radial diffusion coefficient $D_\perp$ is given as

$$D_\perp=-\frac{\Gamma}{\frac{\partial N}{\partial r}}. \tag{11}$$

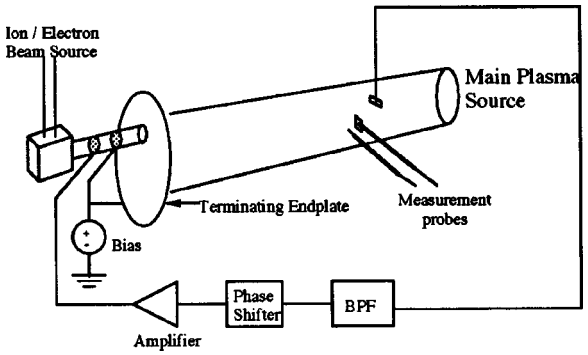


FIG. 1. Schematic of the experimental setup of the feedback experiment. The measurement probes are a Langmuir probe biased to collect ion saturation current, which measures the density fluctuation, and a capacitive probe which measures floating potential fluctuations. BPF denotes a bandpass filter used to eliminate unwanted noise.

As the radial electric field induced rotation is responsible for this instability, a convenient experimental control knob is the end plate bias in CLM which determines the electric field and ultimately the fluctuation levels and transport. As mentioned before, we measure $\tilde{n}$ via Langmuir probe biased at ion saturation current. As the plasma potential $\tilde{\phi}_p$ is not directly measurable, we assume that in our plasma with a significant population of hot electrons, the following relation between floating potential $\tilde{\phi}_f$ (which is measurable) and plasma potential $\tilde{\phi}_p$ can be used[24]:

$$\tilde{\phi}_p=\tilde{\phi}_f+E_{\mathrm{hot},e},$$

where $E_{\mathrm{hot},e}$ is the energy of hot electrons in volts. Figure 2(a) shows the reduction of density fluctuation levels under feedback, while Fig. 2(b) shows the same for potential fluctuation levels. The radial particle flux is obtained from averaging 100 cross-power spectrum samples. The experiments were repeated for various end plate biases to yield different fluctuation power spectra and radial flux. The diffusion coefficients $D_\perp$ were then computed using Eqs. (10) and (11) for various end plate biases and plotted versus the corresponding fluctuation level $\tilde{n}$ in Fig. 3, without and with feedback. It clearly shows that feedback uniformly reduces the anomalous diffusion coefficient over the whole range. This figure is extremely interesting in that it clearly shows that the scaling of the diffusion coefficient $D_\perp$ vs density fluctuation level $\tilde{n}/N$ is linear both without and with feedback. As our linear feedback used here can only affect the linear growth rate of the mode, it is clear from the figure that feedback does not alter the nonlinear dynamics of the mode, which presumably determines the transport scaling. Furthermore, one may conclude that the transport scaling in this case is of strong turbulence type $(\sim\tilde{n}/N)$. Even though from

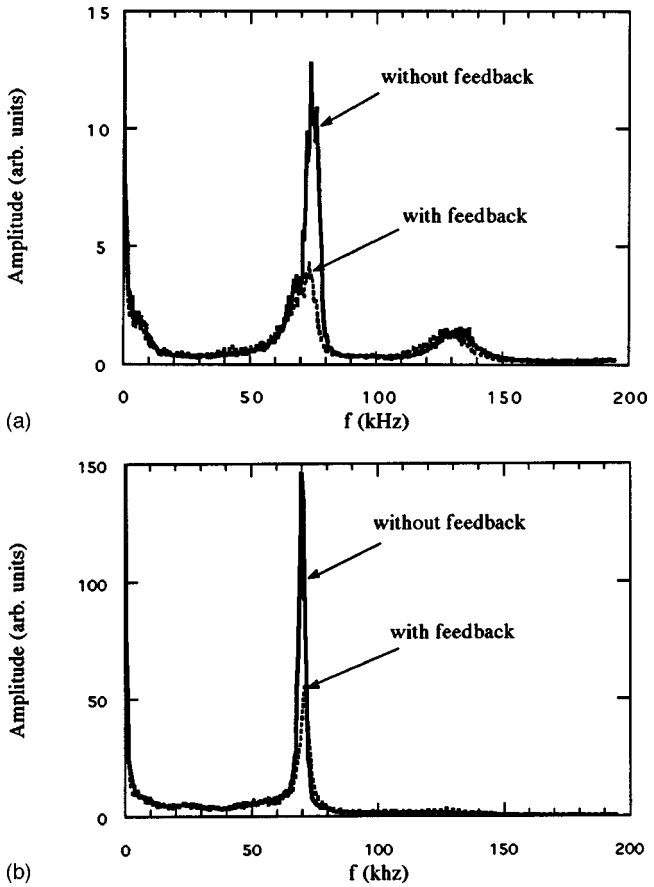


FIG. 2. (a) Reduction of density fluctuations. Typical fluctuation spectra, with and without feedback suppression. (The area under the peak was integrated to obtain the points on the graph.) (b) Reduction of potential fluctuations. Typical fluctuation spectra, with and without feedback suppression. (The area under the peak was integrated to obtain the points on the graph.)

the typical spectrum of Fig. 2(a) there is apparently only one mode, in fact there are several three-wave coupling triplets as discussed in the next section. This is in conjunction with the fact that the spectral width of the dominant mode $\Delta\omega \sim \omega$, which is the frequency of the mode in the plasma frame, indicates that we are in a strong turbulence regime. A detailed comparison of these experimental results with various generic theories only is shown in Table I. In view of our data in Fig. 3 and the above remarks, we can say that the only relevant comparisons are with the strong turbulence theories of Dupree[26] and Taylor and McNamara.[29] However, the Taylor and McNamara prediction is nearly an order of magnitude larger than the experimental result. Even though the experimental result is within a factor of 2 and can be considered to be in fairly good agreement with the prediction of Dupree,[26] its applicability in our case is questionable. This is because a primary premise of the theory is the collisional damping of waves enhanced via wave scattering, which is not relevant for the collisionless rotational flute mode in our experiment. Therefore, it is fair to state that there is significant divergence between the experimental results presented here and the present generic theoretical scaling laws of anomalous diffusion. Of course these comments do not apply to more recent sophisticated mode specific theories of anomalous transport due to trapped particle and ion temperature gradient modes. Lastly, the conclusion that linear feedback only reduces the linear drive of an instability and does not alter its nonlinear dynamics will be utilized in the following sections.

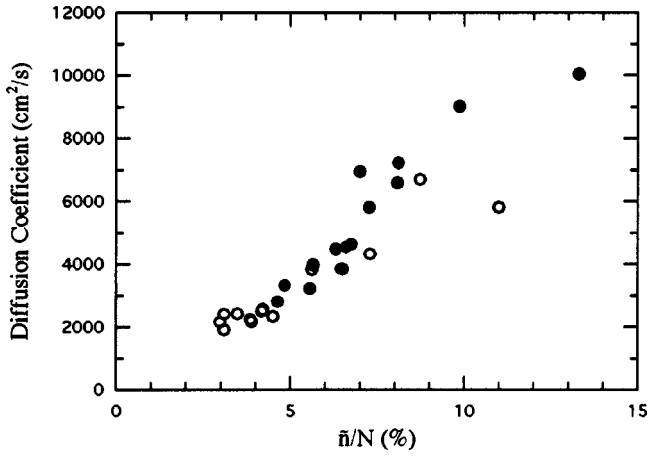


FIG. 3. Diffusion coefficient vs normalized density fluctuation level. Solid dots are cases without feedback, hollow dots are cases with feedback.

### B. Experimental determination of nonlinear dynamic model of plasma fluctuations via feedback

An important part of plasma research has been focused on the difficult problem of developing nonlinear dynamical models of plasma instabilities and fluctuations. The importance derives from the need to understand the essential physics of nonlinear saturation of instabilities, as well as the critical question of anomalous transport. Another reason is that an intelligent design of feedback controller for the suppression of plasma instabilities requires a good model of the nonlinear dynamics of the fluctuations. However, much of the research in this area has been theoretical and at present direct experimental methods are meager. We attempt to study this problem from two perspectives. The first is the determination of the dimension of the attractor in the phase space of fluctuations by a known experimental method. The second is a novel direct experimental method for the determination of a nonlinear dynamic model as discussed below.

#### *1. Search for a low order dynamic model of plasma turbulence*

Recently, there have been attempts to study chaotic dynamics of a variety of nonlinear systems including plasmas. In most research there is a substantial formal hurdle of a very large number of unstable linear modes which must be tracked through their nonlinear evolution. The general question of representing a chaotic dynamical system of large dimensions by a much lower dimensional model is a topic of exciting theoretical, but minimal experimental research in several fields.[32] Particularly in plasma research, low-order attractor dimension has been obtained for magnetospheric dynamic response to solar wind,[33] and tokamak fluctuations.[34] Here we attempt to do a similar study in experiments on an $\mathbf{E}\times\mathbf{B}$ rotational mode discussed in the previous subsection. For this purpose we apply the methods of

TABLE I. Comparison between experimental results and theory.

| Diffusion | ($cm^2/s$) |
|---|---|
| $D_{\perp \exp}$ | $6.5\times10^3=6.5\times10^4(\tilde{n}/N)=0.162(KT_e/eB)\tilde{n}/N$ |
| $D_{\perp \text{classical}}$ | 6.0 |
| Weak turbulence $D_\perp$ : | |
| Quasilinear[a] | $L_n^2\omega_r^2(\tilde{n}/N)^2\sim6.6\times10^6(\tilde{n}/N)^2\sim6.6\times10^4$ |
| Dupree[b] | $L_n^2\omega_r^2\gamma^{-1}(\tilde{n}/N)^2\sim3.0\times10^7(\tilde{n}/N)^2\sim3.0\times10^5$ |
| Kadomtsev[c] | $\gamma/\omega_r\gamma/k_r^2\sim5.6\times10^3$ |
| Gyro-Bohm[d] | $(\rho_i/L_n)(KT_e/eB)\sim8.3\times10^4$ |
| Strong turbulence $D_\perp$ : | |
| Dupree[b] | $k_\theta/k_rKT_e/eB\tilde{n}/N\sim0.32KT_e/eB\tilde{n}N\sim1.28\times10^5\tilde{n}/N$ $\sim1.28\times10^4$ |
| Kadomtsev[c] | $\gamma/k_r^2\sim2.6\times10^4$ |
| Bohm[a] | $1/16KT_e/eB\sim2.5\times10^4$ |
| Taylor & McNamara[c] | $\sqrt{2}KT_e/eB\tilde{n}/N\sim5.6\times10^5\tilde{n}/N\sim5.6\times10^4$ |
| Percolation theory[f,g] | $KT_e/eB(\tilde{n}/N)^{4/7}\sim3.9\times10^5(\tilde{n}/N)^{4/7}\sim1.1\times10^5$ |
| Parameters used: $k_\theta=m/r\sim0.5$, $k_r\sim1.57$, $B=1$ kG, $T_e=4$ eV, $\omega_r=4.7\times10^5$, $\gamma/\omega_r\sim2.2(\tilde{n}/N)$, typ. $\tilde{n}/N\sim0.1$ | |

[a]Reference 25.
[b]Reference 26.
[c]Reference 27.
[d]Reference 28.
[e]Reference 29.
[f]Reference 30.
[g]Reference 31.

chaotic time series analysis of the fluctuation signals, in particular the methods of Grassberger and Procaccia.[35] The time series data are taken from density fluctuation $\tilde{n}$ measured via the fluctuation in the ion saturation current of a Langmuir probe. Using the same probe, a bispectral analysis is also performed to reveal the possible nonlinear saturation mechanism of a three-wave mode coupling involving radial harmonics. Also, time series is taken for cases when the mode is suppressed using an electron beam as described before. The attractor dimension of the time series data is obtained from the Grassberger Procaccia method. For this purpose one can define from a time series data a set of $M$ vectors,

$$Y_i=[y(t_i)y(t_i+\tau)\ldots y(t_i+(N-1)\tau)],$$

where $\tau$ is a time delay and $N$ the embedding dimension. The the number of points $P(\epsilon)$ in a suitable large sphere is

$$P(\epsilon)=\frac{1}{M^2}\sum_{i,j=1}^{M}U(\epsilon-|Y_i-Y_j|);\quad P(\epsilon)\propto\epsilon^d \text{ for small } \epsilon.$$

Here $U$ is a step function, $U(x)=0$ for $x\leqslant0$ and $U(x)=1$ for $x>0$, and $d$ is the dimension of the attractor. Then the slope of $\ln P(\epsilon)$ vs $\ln(\epsilon)$ will be the dimension $d$. This slope is plotted in Figs. 4 and 5 and its value in the saturated regime is identified as the dimension $d$. Even though more advanced techniques exist for improving the signal-to-noise ratio of the time series, we choose to simply bandpass filter the time series using an eighth-order Butterworth filter. Generally, the use of any time or frequency domain based filters is discouraged, such as discussed in Mitschke *et al.*[36] However, we believe that our chaotic system differs from other typical systems in a very significant way, namely that the signal of interest for our case is the $\mathbf{E}\times\mathbf{B}$ mode, which is concentrated in a narrow region of the frequency spectrum, whereas most other low-dimensional chaotic systems have very broad spectral content. By filtering out signal far away from the mode spectrum, we believe that other signals and chaotic dynamics unrelated to $\mathbf{E}\times\mathbf{B}$ instability which are not of our interest can be separated from the real attractor dimension of the $\mathbf{E}\times\mathbf{B}$ modes. Figure 4 shows the result of this after applying bandpass filters with cutoff frequencies at 10 and 200 kHz. One can clearly see that all the curves are converging to a dimension close to three. The same procedure is performed when the mode is suppressed with feedback. The resulting attractor dimension, which is shown in Fig. 5, is almost identical to the case without feedback.

Now we discuss a physical rationale for the result of the attractor dimension of 3. Even though there is only one dominant ($m=1,n=0,k_\parallel=0$) in the fluctuation spectrum of Fig. 2, we have found in a previous study using bicoherence to search for three-wave coupling, a radial harmonic ($m=1,n=1$) hiding in this dominant feature and a small amplitude $m=2$, $n=0$ near the second harmonic frequency in the spectrum. Here, $m$, $n$, and $k_\parallel$ are the azimuthal, radial,

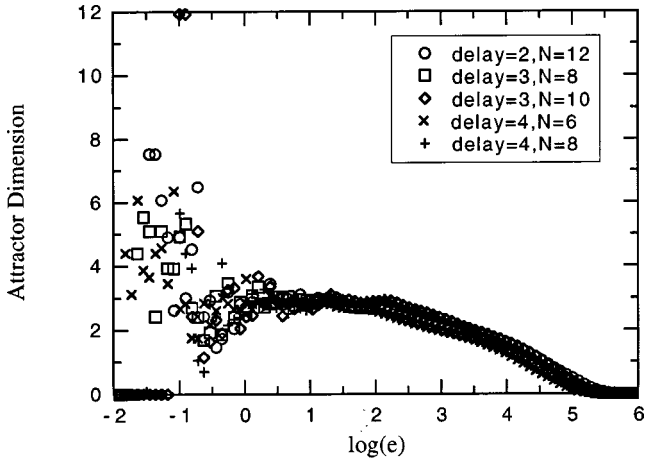


FIG. 4. Attractor dimension vs $\ln(\epsilon)$ of $\mathbf{E}\times\mathbf{B}$ mode for different embedding dimensions $N$ after application of a bandpass filter with cutoff frequencies at 10 and 200 kHz.

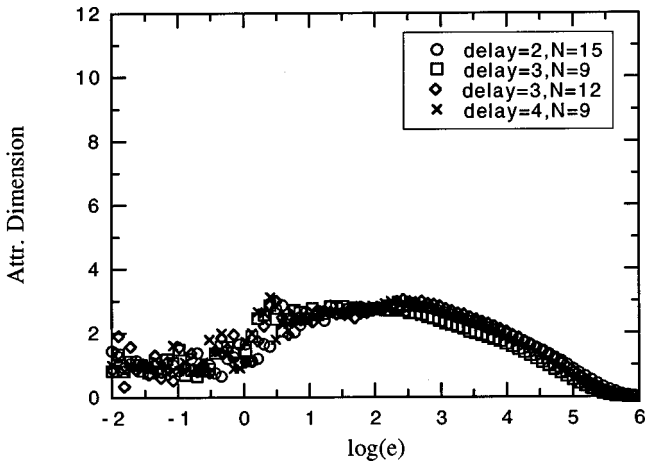


FIG. 5. Attractor dimension vs $\ln(\epsilon)$ of $\mathbf{E}\times\mathbf{B}$ mode after feedback suppression and application of a bandpass filter with cutoff frequencies at 10 and 200 kHz.

and axial wave numbers, respectively. Therefore, nonlinear saturation occurs via a three-mode coupling process. In one limit of a three-wave mode coupling model with only weak correlation one may expect three independent amplitudes and two independent phase differences, leading to an attractor dimension of five. In the other limit of a completely coherent three-mode coupling process, where all the amplitudes and phases are locked, one may expect an attractor dimension of one. However, for an intermediate situation of moderate decorrelations, which may justify random phase approximations (as validated by significant spectral widths), one may expect three independent amplitudes and hence an attractor dimension of three.

### 2. Experimental determination of a nonlinear dynamic model of plasma turbulence using feedback diagnostics

The physics of turbulent transport in plasmas remains largely an open question. An essential ingredient of this physics issue is an experimentally validated nonlinear dynamical model of plasma turbulence. Direct experimental determination of the nonlinear dynamics underlying the turbulence is nearly an intractable proposition. Experimental verification of a number of well-known theoretical dynamical models is largely absent. Here we describe a novel experimental method for the determination of the parameters of a three-wave coupling model which is an often used theoretical tool. The method is based on Ritz, Powers, and Bengston,[37] which assumes a nonlinear three-wave coupling equation in the form of

$$\frac{\partial\phi(k,t)}{\partial t}=(\gamma_k+i\omega_k)\phi(k,t)+\frac{1}{2}\sum_{k=k_1+k_2}\Lambda_k^Q(k_1,k_2)\times\phi(k_1,t)\phi(k_2,t), \tag{12}$$

where the spatial Fourier spectrum $\phi(k,t)$ of the fluctuating field is defined by $\phi(x,t)=\Sigma_k|\phi(k,t)|e^{i(\theta(k,t)+kx)}$ [slow varying amplitude with respect to phase changes in $\theta(k,t)$], $\gamma_k$ denotes the growth rate, $\omega_k$ the real frequency, and $\Lambda_k^Q(k_1,k_2)$ the coupling coefficient of this process. After discretization and transforming to the frequency domain, Eq. (12) is multiplied by $\Phi_\omega^*$ and $\Phi_{\omega_1}^*\Phi_{\omega_2}^*$, respectively, and ensemble averaged, yielding

$$\langle\Phi_\omega(\tau)\Phi_\omega^*\rangle=L_\omega\langle\Phi_\omega\Phi_\omega^*\rangle+\frac{1}{2}\sum_{\omega=\omega_2+\omega_1}Q_{\omega_1,\omega_2}\times\langle\Phi_{\omega_1}\Phi_{\omega_2}\Phi_\omega^*\rangle, \tag{13}$$

$$\langle\Phi_\omega(\tau)\Phi_{\omega_1'}^*\Phi_{\omega_2'}^*\rangle=L_\omega\langle\Phi_\omega\Phi_{\omega_1'}^*\Phi_{\omega_2'}^*\rangle+\frac{1}{2}\sum Q_{\omega_1,\omega_2}\times\langle\Phi_{\omega_1}\Phi_{\omega_2}\Phi_{\omega_1'}^*\Phi_{\omega_2'}^*\rangle, \tag{14}$$

where $L_\omega=(\gamma_k+i\omega_k)\tau+1-i[\theta(k,t,+\tau)-\theta(k,t)]/e^{-i[\theta(k,t+\tau)-\theta(k,t)]}$ and $Q_{\omega_1,\omega_2}=\Lambda_k^Q(k_1,k_2)\tau/e^{-i[\theta(k,t+\tau)-\theta(k,t)]}$ can be solved for from Eqs. (13) and (14) with experimental data. One prerequisite of this approach is obtaining the fourth-order moment $\langle\Phi_{\omega_1}\Phi_{\omega_2}\Phi_{\omega_1'}^*\Phi_{\omega_2'}^*\rangle$, which is computationally intensive. This is solved by Ritz *et al.* by approximating the fourth-order moment with second-order moments $\langle|\Phi_{\omega_1}\Phi_{\omega_2}|^2\rangle$ by neglecting terms $(\omega_1',\omega_2')\neq(\omega_1,\omega_2)$. Since the fluctuations in CLM are mostly narrow band with distinct frequency peaks, one can easily identify discrete three-wave coupling triplets with distinct $k$ numbers, as opposed to the broadband turbulence present in many other devices. Furthermore, in the past we have performed several experiments using feedback from an ion/electron beam source,[5,6] or even a Langmuir probe, which enabled us to suppress/enhance the underlying linear drive of the instability.[11] If fact, in this experiment we make novel exploitation of this feedback system to avoid calculating the fourth-order moments. We include linear feedback in Eq. (12) by adding $G\phi(k,t)$ on the right-hand side, where $G$ is the complex (constant) gain of the feedback loop. It can be seen that $G$ only modifies the linear operator of Eq. (12), such that Eq. (13) can be rewritten as

$$\langle\Phi_\omega(\tau)\Phi_\omega^*\rangle'=\left(L_\omega+\frac{G}{e^{-i[\theta(k,t+\tau)-\theta(k,t)]}}\right)\langle\Phi_\omega\Phi_\omega^*\rangle'+\frac{1}{2}\sum Q_{\omega_1,\omega_2}\langle\Phi_{\omega_1}\Phi_{\omega_2}\Phi_\omega^*\rangle', \tag{15}$$

where the prime denotes data from another experiment different from that implied in Eq. (14). By experimentally adjusting for different feedback gain $G$, and measuring the subsequent fluctuation signal, we can generate an arbitrary number of equations with a fixed number of unknowns. This, in principle, allows us to solve for $\gamma_k+i\omega_k$ and the coupling coefficients $\Lambda_k^Q(k_1,k_2)$ for each particular mode $k$.

The mode used for this experiment is again the centrifugal flute mode driven by the $\mathbf{E}\times\mathbf{B}$ rotation of the plasma discussed in the above sections. With somewhat different parameters for the experiment, the dominant mode has azimuthal mode number $m=1$, with typical frequency $f=50$ kHz shown in Fig. 6 and broad radial extent equivalent to an $n=0$ harmonic in radius. Also present, but usually at a few kHz higher than the dominant mode, is a mode which

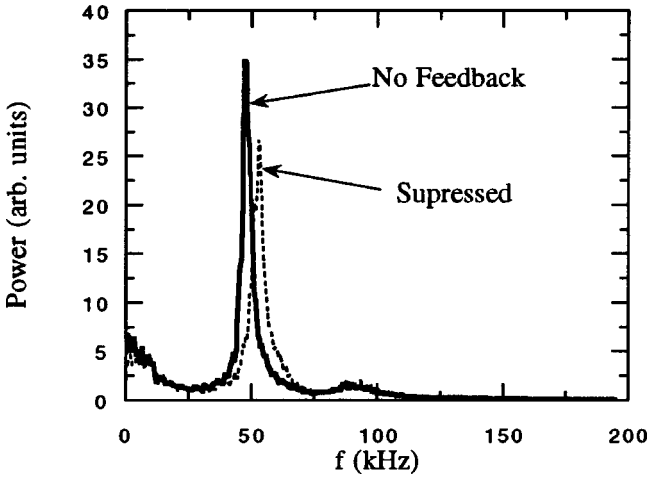


FIG. 6. Power spectrum of plasma instabilities present in CLM. Two cases are provided, one with moderate feedback suppression and one with feedback turned off.

shows a radial structure consistent with an $n=1$ harmonic, as previously discovered and discussed.[39] Even though the $n=1$ radial harmonic is not directly evident from the frequency spectrum, its existence becomes apparent when the three-wave coupling triplets are being identified. This can be seen from the bicoherence contour plot shown in Fig. 7, which measures the second-order correlation of three waves with frequency $f_1$, $f_2$, and $f_1+f_2$, where $f_1$ and $f_2$ are plotted on the $x$ and $y$ axis, respectively. The coupling of the dominant mode with the higher radial harmonic can be seen from the close up view of the previous plot in Fig. 8. Several sets of coupling triplets can be identified from the plot and shown in Table II.

First, we estimate the real frequencies $\omega_k$ from bicoherence and the power spectrum. Then, to determine the growth rate and coupling coefficients, only the real part of Eq. (15) is used, since it is numerically more stable to do so. Equation (15) is further modified by letting $e^{i[\theta(k,t+\tau)-\theta(k,t)]} \simeq \langle \Phi_\omega(\tau)\Phi_\omega^* \rangle / |\langle \Phi_\omega(\tau)\Phi_\omega^* \rangle| \simeq e^{i\omega\tau}$,

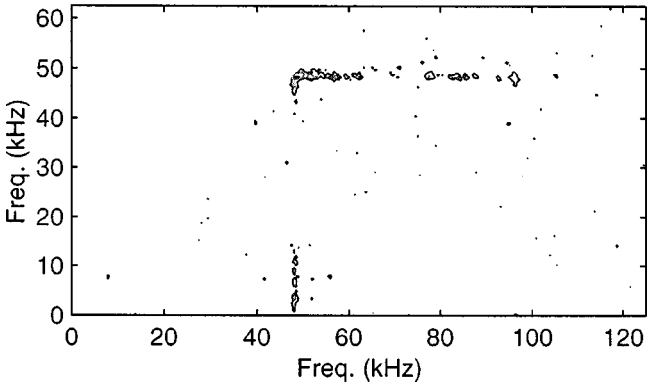


FIG. 7. Bicoherence contour plot of the plasma instability. Each contour step corresponds to bicoherence of 0.06. Due to symmetry properties, only the lower diagonal half is displayed. Peaks on the diagonal represent self coupling to its harmonic, whereas peaks offset from the diagonal represent coupling of two separate modes.

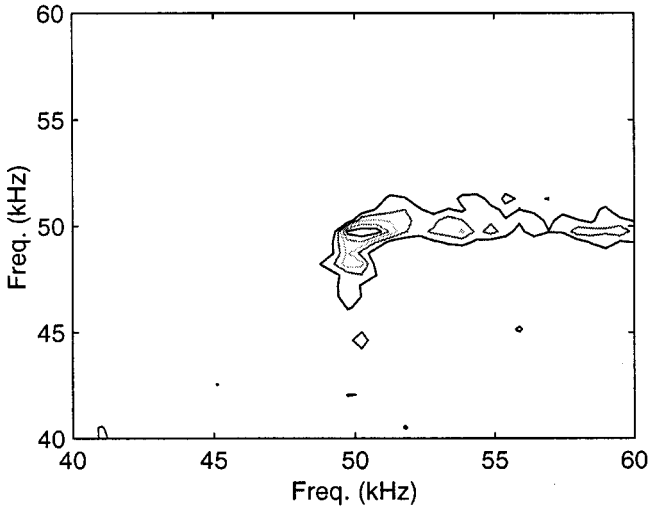


FIG. 8. Closeup of Fig. 7. The contour extending off the diagonal represents coupling of the dominant mode with a ''radial'' harmonic close by in frequency. Each contour line represents an increase of value by 0.06.

$$|\langle \Phi_\omega(\tau)\Phi_\omega^* \rangle'| = [(\gamma_k - |G|\cos\theta)\tau + 1)\langle \Phi_\omega \Phi_\omega^* \rangle' + \mathrm{Re}\left\{ \frac{1}{2} \sum \Lambda_k^Q(k_1,k_2)\tau \langle \Phi_{\omega_1}\Phi_{\omega_2}\Phi_\omega^* \rangle' \right\}. \quad (16)$$

All the above quantities related to the fluctuation signal $\Phi_\omega$ are obtained by measuring the density fluctuation using a Langmuir probe biased to collect ion saturation current, and then performing the appropriate mathematical functions once the signal was digitized to 12 bits accuracy. Since all the modes have some spectral width, the power of the modes is integrated over the appropriate frequency band, after they have been ensemble averaged over 200 samples. The feedback setup is almost identical to that described in Sec. III above, except that actuator/suppressor consists of a separate Langmuir probe for convenience, even though our ion/electron beam provides similar results. After appropriate calibrations, the magnitude of the gain is kept constant, and the phase is adjusted to obtain the different sets of equations. In order to avoid solving for excessively insignificant coupling coefficients, some triplets are truncated or omitted. This include all triplets where two out of the three modes exhibit low power, such as the coupling of the dominant mode with the mode at 80–100 kHz to a third mode at above 120 kHz. This is possible because for the actual calculation, the bispectrum is needed instead of the normalized bicoherence, such that low mode amplitude results in low bispectrum. Also, in theory the self coupling of the mode at $f$ and the coupling with the radial harmonic at $(f+\Delta f)$ couples to two independent modes at $2f$ and $(2f+\Delta f)$, respectively. In reality, it is impossible to accurately distinguish these two modes, as the mode power at these frequencies again is quite small. Therefore, these two modes at $2f$ and $(2f+\Delta f)$ are lumped together and considered as a ''single'' mode. Finally, one should note that since the bispectrum is needed

TABLE II. Table showing growth rate $\gamma$ (Hz) and coupling coefficient $\Lambda$ (V/s$^{-1}$) related to each mode.

| | | | | |
|---|---|---|---|---|
| For mode $k$: $f=50$ kHz, $m=1$, $n=0$ flute mode: | | | | |
| $\gamma_k=2106$, | $\mathbf{Re}\{\Lambda_k^Q(k,k_2)\}=561$, | $\mathbf{Im}\{\Lambda_k^Q(k,k_2)\}=163$, | $\mathbf{Re}\{\Lambda_k^Q(k_1,k_2)\}=-3699$, | $\mathbf{Im}\{\Lambda_k^Q(k_1,k_2)\}=6712$. |
| | $\mathbf{Re}\{\Lambda_k^Q(k_1,k_3)\}=-117$, | $\mathbf{Im}\{\Lambda_k^Q(k_1,k_3)\}=941$. | | |
| For mode $k_1$: $f=55$ kHz, $m=1$, $n=1$ flute mode: | | | | |
| $\gamma k_1=-2492$, | $\mathbf{Re}\{\Lambda_{k_1}^Q(k,k_2)=-2809\}$ | $\mathbf{Im}\{\Lambda_{k_1}^Q(k,k_2)\}=938$, | $\mathbf{Re}\{\Lambda_{k_1}^Q(k,k_3)\}=-615$, | $\mathbf{Im}\{\Lambda_{k_1}^Q(k,k_3)\}=632$. |
| For mode $k_2$: $f\simeq 102$ kHz, $m=2$, $n=0$ flute mode: | | | | |
| $\gamma k_2=-16\,542$, | $\mathbf{Re}\{\Lambda_{k_2}^Q(k,k)\}=153$, | $\mathbf{Im}\{\Lambda_{k_2}^Q(k,k)\}=270$, | $\mathbf{Re}\{\Lambda_{k_2}^Q(k,k_1)\}=-634$, | $\mathbf{Im}\{\Lambda_{k_2}^Q(k,k_1)\}=-3560$. |
| For mode $k_3$: $f\simeq 5$ kHz drift wave: | | | | |
| $\gamma k_3=-909$, | $\mathbf{Re}=\{\Lambda_{k_3}^Q(k,k_1)\}=401$, | $\mathbf{Im}\{\Lambda_{k_3}^Q(k,k_1)\}=-75$. | | |

instead of the bicoherence, in most cases high bispectrum values are obtained despite low bicoherence results. Hence, as long as the coupling triplets can be correctly identified from one of the cases, low bicoherence in other cases does not necessarily indicate poor bispectrum results.

It is found that the bicoherence readings are far better during feedback enhancement than during suppression, mostly due to the increased signal-to-noise ratio from enhancement. Therefore, data are taken at seven different phase settings, all of which provide enhancement of the mode. These, along with the case of not applying any feedback, provide eight independent equations. They are then used to solve for all the unknowns. Since even the dominant mode has the highest number of only seven unknowns, Singular Value Decomposition is used to solve for the unknowns. The result is summarized in Table II and discussed below. First, it is noted that the dominant mode $k$ has positive growth rate, while the two other possible members of a triad have negative growth (damping) rates. This is certainly consistent with the physics requirement that for the nonlinear saturation of a growing mode, one needs coupling to damped modes which provide the energy sinks for the establishment of a steady state. Preliminary results of a detailed but approximate theory indicate rough agreement with the experimental results presented in Table II.

Lastly, it is noted that a recent theoretical/experimental method[38] using a modified Ritz method can substantially improve the results. However, it relies on a calculation of fourth-order moments, which can be avoided by our method utilizing feedback.

## ACKNOWLEDGMENTS

This work was supported by the National Science Foundation Grant No. EC-96-10153, and Department of Energy Grant No. DE-FG-02-87ER532E7.

[1] A. K. Sen, Phys. Fluids **18**, 1187 (1975).
[2] A. K. Sen, IEEE Trans. Plasma Sci. **PS-7**, 116 (1979).
[3] A. Sekiguchi, A. K. Sen, and G. A. Navratil, IEEE Trans. Plasma Sci. **PS-18**, 685 (1991).
[4] A. Sekiguchi, A. K. Sen, P. Tham, G. A. Navratil, and R. G. Greaves, Rev. Sci. Instrum. **63**, 4227 (1992).
[5] P. Tham, A. K. Sen, A. Sekiguchi, and G. A. Navratil, Phys. Rev. A **67**, 204 (1991).
[6] P. Tham and A. K. Sen, Phys. Rev. A **46**, R4520 (1992).
[7] A. K. Sen, J. Plasma Phys. **20**, 1 (1978).
[8] A. K. Sen, IEEE Trans. Autom. Control. **24**, 272 (1979).
[9] M. Ghassemi and A. K. Sen, Plasma Phys. **23**, 273 (1981).
[10] M. Ghassemi and A. K. Sen, IEEE Trans. Plasma Sci. **PS-9**, 41 (1981).
[11] A. B. Plaut, A. K. Sen, G. A. Navratil, and R. Scarmozzino, Phys. Fluids B **1**, 293 (1989).
[12] A. W. Morris, T. C. Hender, J. Hugill, P. S. Haynes, P. C. Johnson, B. Loyd, D. C. Robinson, and C. Sylvester, Phys. Rev. Lett. **64**, 1254 (1990).
[13] R. Fitzpatrick, Phys. Plasmas **4**, 2519 (1997).
[14] G. A. Navratil, Phys. Plasmas **9**, 1855 (1998).
[15] A. M. Garofalo, A. D. Turnbull, E. J. Scott *et al.*, Phys. Plasmas **6**, 1893 (1999).
[16] A. K. Sen, Phys. Rev. Lett. **76**, 1252 (1996).
[17] A. K. Sen, R. Singh, A. Sen, and P. K. Kaw, Phys. Plasmas **4**, 3217 (1997).
[18] *Feedback and Dynamic Control of Plasmas*, edited by T. K. Chu and H. Hendel (American Institute of Physics, New York, NY, 1970).
[19] A. K. Sen, Phys. Plasmas **1**, 1479 (1994).
[20] D. G. Luernberger, IEEE Trans. Autom. Control. **AC-11**, 190 (1966).
[21] G. A. Navratil, J. Slough, and A. K. Sen, Plasma Phys. **24**, 184 (1982).
[22] T. D. Rognlien, J. Appl. Phys. **44**, 3505 (1973).
[23] J. S. Chiu and A. K. Sen, Phys. Plasmas **4**, 2933 (1997).
[24] N. Hershkowitz, *Plasma Diagnostics* (Academic, New York, 1989).
[25] P. C. Liewer, Nucl. Fusion **25**, 543 (1985).
[26] T. H. Dupree, Phys. Fluids **11**, 2680 (1968).
[27] B. B. Kadomtsev, *Plasma Turbulence* (Academic, London, 1965).
[28] F. W. Perkins, C. W. Barnes, D. W. Johnson, S. D. Scott, M. C. Zarnstorff, M. G. Bell, R. E. Bell, C. E. Bush, B. Grek, K. W. Hill, D. K. Mansfield, H. Park, A. T. Ramsey, J. Schivell, B. C. Stratton, and E. Synakowski, Phys. Fluids B **5**, 477 (1993).
[29] J. B. Taylor and B. McNamara, Phys. Fluids **14**, 1492 (1971).
[30] Y. B. Zel'dovich, Sov. Phys. JETP Lett. **38**, 57 (1983).
[31] A. V. Gruzinov, M. B. Isichenko, and J. Kalda, Sov. Phys. JETP **70**, 263 (1990).
[32] A. Lichtenberg and M. Lieberman, Regular and Chaotic Dynamics (Springer Verlag, New York, 1991), p. 591.
[33] D. A. Roberts, D. N. Baker, and A. J. Klimas, Geophys. Res. Lett. **18**, 151 (1991).
[34] M. Persson and H. Nordman, Phys. Rev. D **67**, 3396 (1991).
[35] P. Grassberger and I. Procaccia, Physica (Utrecht) **9**, 189 (1983).
[36] F. Mitschke, M. Möller, and W. Lange, Phys. Rev. A **37**, 4518 (1988).
[37] Ch. P. Ritz, E. J. Powers, and R. D. Bengston, Phys. Fluids B **1**, 153 (1989).
[38] J. S. Kim, R. J. Fonck, R. D. Durst, P. W. Terry, E. Fernandez, and A. Ware, Phys. Plasmas **3**, 3998 (1996).
[39] P. Tham and A. K. Sen, Phys. Plasmas **1**, 3577 (1994).